SUPPORTING INFORMATION

Gene expression in cytomimetic protocells is most efficient at physiological crowding conditions

Mahesh A. Vibhute, Mark H. Schaap, Roel J. M. Maas, Frank H.T. Nelissen, Evan Spruijt, Hans A. Heus, Maike M. K. Hansen*, Wilhelm T. S. Huck*.

Radboud University, Institute for Molecules and Materials, Heyendaalseweg 135, 6525 AJ Nijmegen, The Netherlands

*Corresponding Authors: Maike M. K. Hansen (maike.hansen@ru.nl), Wilhelm T. S. Huck (w.huck@science.ru.nl)

CONTENTS

1. Diffusion measurements

1.1 Diffusion coefficients

1. GFP diffusion

A. IVTT	
Lysate (mg/ml)	Diffusion coefficient (D_{GFP}) (um^2s^{-1})
73	35.2 ± 3.6
78	20.9 ± 1.5
94	26.4 ± 2.1
104	13.4 ± 0.9
106	21.1 ± 2.0
107	24.2 ± 2.4
117	27.55 ± 2.7
118	16.2 ± 1.3
120	18.8 ± 1.6
126	11.4 ± 0.9
138	9.3 ± 0.6
141	12.3 ± 0.9
143	8.1 ± 0.6
145	16.9 ± 1.6
148	14.4 ± 1.1
153	15.2 ± 1.3
155	8.9 ± 0.6
156	18.9 ± 1.7
158	10.9 ± 0.8
160	11.0 ± 0.8
164	11.5 ± 0.9
166	13.3 ± 1.1
168	3.4 ± 0.2
168	9.6 ± 0.8
170	14.3 ± 1.1
171	7.2 ± 0.6
172	3.0 ± 0.3
172	26.2 ± 2.1
175	10.8 ± 0.8
194	9.6 ± 0.3
202	6.8 ± 0.6
258	7.2 ± 0.6
294	15.9 ± 1.2
328	2.0 ± 0.1
334	1.8 ± 0.1

B. No FB, with HEPES (pH 8)	
Lysate (mg/ml)	D_{GFP} (um^2s^{-1})
109	15.0 ± 1.3
110	14.5 ± 1.3
114	14.7 ± 1.2
124	12.2 ± 1.0
141	7.4 ± 0.4
146	8.8 ± 0.6
150	9.7 ± 0.7
168	10.1 ± 0.7
189	2.9 ± 0.19
190	7.6 ± 0.6
230	1.9 ± 0.1
235	4.5 ± 0.3
287	3.2 ± 0.2
291	1.67 ± 0.08
298	3.0 ± 0.16
302	1.9 ± 0.13
309	1.7 ± 0.07
325	1,7 ± 0.09
334	0.95 ± 0.03
391	1.31 ± 0.09

C. No FB, no HEPES	
Lysate (mg/ml)	D_{GFP} (um^2s^{-1})
91	28.3 ± 1.9
93	28.3 ± 1.99
101	20.5 ± 1.8
107	20.0 ± 1.1
117	22.8 ± 1.57
133	7.1 ± 0.8
134	5.1 ± 0.4
136	5.0 ± 0.3
144	14.4 ± 1.0
145	13.5 ± 0.8
153	5.2 ± 0.4
190	4.4 ± 0.3
191	1.9 ± 0.09
195	5.0 ± 0.3
205	0.59 ± 0.02
206	0.47 ± 0.01
207	0.69 ± 0.04
207	3.1 ± 0.2
215	0.46 ± 0.01
225	0.68 ± 0.02
229	0.44 ± 0.01

A. No FB, with HEPES (pH 6)

Lysate (mg/ml)	D_{GFP} (um^2s^{-1})
68	18 ± 6.4
70	17.3 ± 6.6
107	17.5 ± 5.8
109	22.8 ± 5.4
136	2.9 ± 0.16
152	1.6 ± 0.1
161	1.4 ± 0.07
165	1.3 ± 0.18
166	1.2 ± 0.04
171	1.5 ± 0.08
181	1.5 ± 0.22
213	1 ± 0.05
219	1.9 ± 0.17
221	1.4 ± 0.27
224	1.2 ± 0.14
119	0.14 ± 0.07
121	0.28 ± 0.02
124	0.44 ± 0.04
125	0.27 ± 0.02
135	0.15 ± 0.007
135	0.30 ± 0.03
140	0.40 ± 0.04
142	0.20 ± 0.01
169	0.21 ± 0.02
169	0.15 ± 0.01
173	0.20 ± 0.02
178	0.18 ± 0.02
183	0.08 ± 0.004
183	0.16 ± 0.01
194	0.20 ± 0.02
198	0.076 ± 0.004
200	0.084 ± 0.004
232	0.098 ± 0.005
232	0.047 ± 0.003

Table S1. Diffusion coefficients of GFP determined at different lysate concentrations in four different conditions. The corresponding SD values were calculated by estimating the uncertainties in fit parameters (See Methods). [GFP] = 10 μm.

2. Atto488 labelled 70S ribosomes diffusion

A. IVTT	
Lysate (mg/ml)	D_{70S} (um^2s^{-1})
108	0.71 ± 0.05
130	0.47 ± 0.04
133	0.37 ± 0.03
135	0.40 ± 0.04
144	0.46 ± 0.03
158	0.30 ± 0.02
174	0.15 ± 0.01
177	0.25 ± 0.02
178	0.22 ± 0.01
205	0.19 ± 0.01
215	0.101 ± 0.008
239	0.077 ± 0.007

B. No FB, with HEPES	
Lysate (mg/ml)	D_{70S} (um^2s^{-1})
91	0.38 ± 0.02
116	0.42 ± 0.04

C. No FB, no HEPES	
Lysate (mg/ml)	D_{70S} (um^2s^{-1})
95	0.13 ± 0.01
101	0.08 ± 0.01
104	0.12 ± 0.01
142	0.17 ± 0.01
192	0.09 ± 0.01
196	0.07 ± 0.01
202	0.051 ± 0.004
234	0.082 ± 0.007
245	0.102 ± 0.008
267	0.034 ± 0.003
278	0.049 ± 0.004

Table S2. Diffusion coefficients of Atto488 labelled 70S ribosomes determined at different lysate concentrations in three different conditions. The ribosomes were labelled according to protocol optimized from literature (See below). The corresponding SD values were calculated by estimating the uncertainties in fit parameters (See Methods). [Ribosomes] = 0.21 μM.

3. NBD-Glucose diffusion

Lysate (mg/ml)	D_{NBDG} (um^2s^{-1})
251	51.1 ± 8.6
278	51.4 ± 8.5
324	38.6 ± 6.1
327	34.8 ± 5.8
336	52.3 ± 7.1
344	26.6 ± 3.9
370	32.8 ± 4.4

Table S3. Diffusion coefficients of NBDG determined in presence of deCFP expression. The corresponding SD values were calculated by estimating the uncertainties in fit parameters (See Methods). [NBDG] = 200 μM.

1.2 Ribosome labelling

Sucrose gradient purified E. coli BL21 70S ribosomes were labelled using a protocol optimized from literature.[1,2] The labelling reaction was conducted in a buffer with the following composition: 50 mM Tris-HCl, pH 7.6, 15 mM $MgCl_2$, 100 mM NH_4Cl and 6 mM β-mercaptoethanol, containing 4.8 μM of ribosomes and 250 μM ATTO488 NHS-ester (ATTO-TEC GmbH). The reaction mixture was incubated at 37°C for 30 minutes and any formed precipitate was removed by centrifugation for 1 minute at 10 krpm in a tabletop centrifuge. The supernatant containing ribosomes was concentrated in a spin column (Vivaspin 6, MWCO 30 kDa) and thoroughly washed with the labelling buffer to remove the excess of dye. The final concentration of labelled ribosomes was estimated at 5.1 μM, and the label concentration to be 27.5 μM using a Nanodrop 1000 (Isogen). This corresponds to ~5-6 labels per ribosome. The ribosomes were then flash frozen with liquid nitrogen and stored at -80°C until further use.

1.3 GFP isolation

A 25 ml starter culture of *Escherichia coli* BL21(DE3)pLysS containing pET15b-His_6-GFP was grown overnight at 37°C in 2xYT medium containing ampicillin (100 μg/ml) and chloramphenicol (30 μg/ml) while shaking. The dense-grown culture was used to inoculate 1L of the same medium and grown at 30°C while shaking. Upon reaching a density of OD_{600}=0.4, GFP expression was induced by adding IPTG to a final concentration of 1 mM and cultivation was continued for 4.5 hours. Cells were harvested by centrifugation at 5000 rpm in a Beckman JA-10 rotor at 4°C for 10 minutes and the pellet was stored overnight at -80°C. Next day, the pellet was resuspended in ice-cold lysis buffer (50 mM sodium phosphate buffer, 300 mM NaCl, 5 mM β-mercaptoethanol, 0.5 mM EDTA, 20 mM imidazole, 0.5 mg/ml lysozyme, pH 8.0) and sonicated on ice at maximum amplitude (MSE Soniprep 150) for 4 cycles of 30 seconds with 60 seconds pause intervals. The lysate was centrifuged at 15000 rpm in a Beckman JA-20 rotor at 4°C for 45 minutes. The cleared lysate was then loaded onto a pre-equilibrated (buffer see below) 5 ml His-Trap HP column in a cold room. The column was successively washed with 25 ml of column equilibration buffer (identical to lysis buffer, but without EDTA and lysozyme) and 25 ml of washing buffer (50 mM sodium phosphate buffer, 300 mM NaCl, 5 mM β-mercaptoethanol, 50 mM imidazole, pH 8.0). His_6-tagged GFP was eluted with elution buffer (50 mM sodium phosphate buffer, 300 mM NaCl, 5 mM β-mercaptoethanol, 300 mM imidazole, pH 8.0) and fractions of 1.5 ml were collected. Fractions containing GFP were pooled and dialyzed overnight at 4°C against 2 litres of 25 mM sodium phosphate buffer, 0.5 mM DTT, 0.1 mM EDTA, pH 8.0. The purified GFP was then aliquoted, flash frozen with liquid nitrogen and stored at -80°C.

1.4 Lysate concentration estimation by BCA assay

The protein content of lysate was determined to be 44 mg/ml (± 6 mg/ml) using Pierce BCA assay.

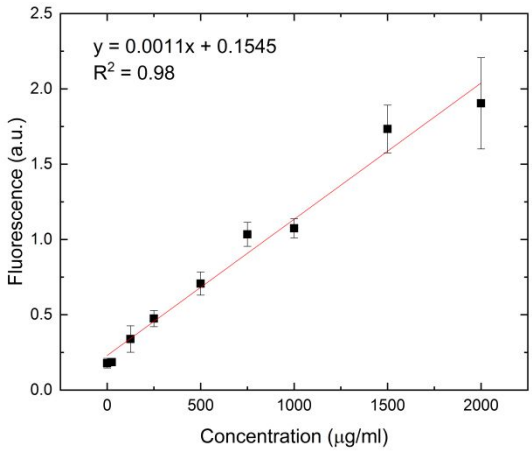

Figure S1. BCA assay calibration curve to determine the concentration of proteins in lysate. The data points correspond to mean ± SD (n=2).

1.5 Encapsulation accuracy

In order to verify that there is no loss of contents during encapsulation and osmotic shrinkage, we performed control experiments to measure the accuracy of these processes. We encapsulated the components of the reaction mixture along with eGFP in partially dewetted liposomes and osmotically shrank them to different extents. We then measured the total fluorescence intensities of eGFP in these liposomes. Any loss of fluorophore during osmotic shrinkage would lead to variation in the total fluorescence intensity (I_{eGFP}) detected in these liposomes. We found no significant variation in the total fluorescence intensity (Figure S2). The CV corresponding to the total fluorescence intensity in these measurements amounted to 5%. We therefore, concluded that there was no significant loss of contents during osmotic shrinkage.

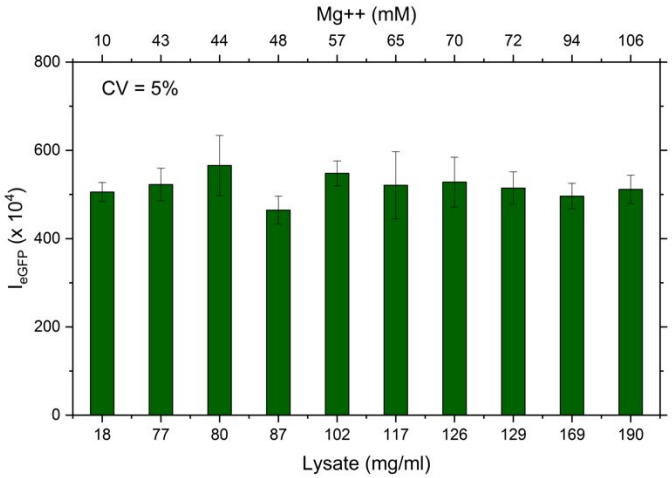

Figure S2. The total fluorescence intensity corresponding to eGFP in shrunk liposomes remains the same, indicating that there is no loss of contents due to osmotic shrinkage. The error bars indicate SD over liposomes imaged corresponding to each lysate concentration (n = 3-7).

It is difficult to achieve exact same macromolecular concentrations over the course of multiple experiments, despite using similar reaction compositions and hypertonic solution concentrations. This renders studying gene expression at specific crowding levels difficult. Therefore, we map expression levels over a wide range of macromolecular concentrations. This involved multiple individual experiments (The data in figure 3 were gathered over the course of 10 experiments). By doing so, we were able to obtain a thin slice of the phase space, and thereby analyse the impact of crowding and magnesium on gene expression efficiency. For details, see below (Section 2.1).

1.6 SNARF measurements

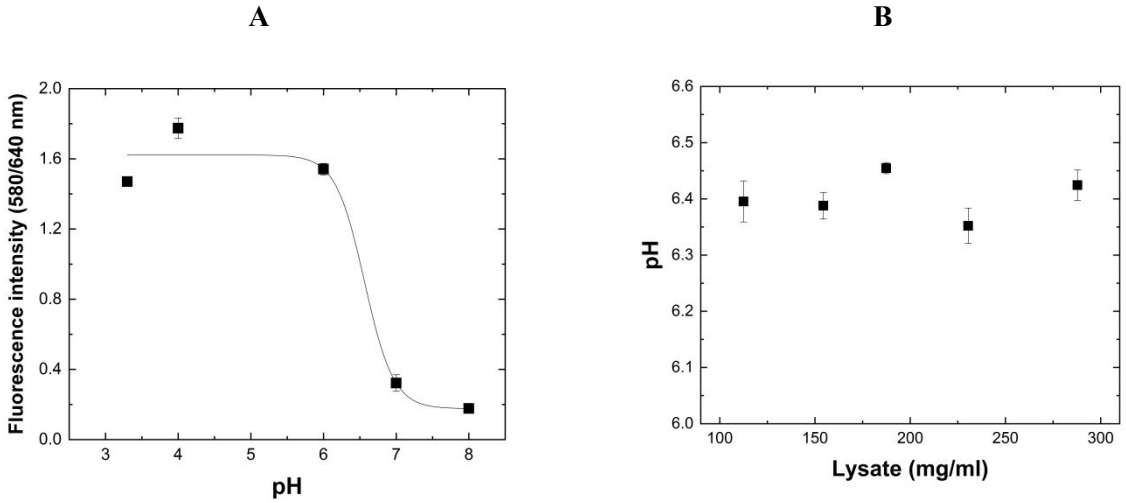

Figure S3. (**A**) Calibration curve for SNARF-5F with sigmoidal fitting. R-square = 0.92. The error bars represent SD calculated for measurements over multiple droplets (n = 9) (**B**) pH determined in shrunk liposomes encapsulated without feeding buffer and HEPES (No FB, no HEPES in Figure 2). The error bars represent SD calculated for measurements over multiple liposomes (n = 2-4)

10 mM SNARF-5F was prepared by dissolving 1mg in 212 ul MQ. Aliquots of 20 ul were prepared and stored at -20°C. For plotting the calibration curve of SNARF-5F, HEPES solutions (0.5M) buffered at different pH (3.34, 4, 7.1 and 8.05) were prepared using acetic acid and 1M KOH. SNARF-5F was added to a final concentration of 0.4 mM. The buffer solutions were then emulsified by vortexing in 2.5% w/v surfactant (RAN biotechnologies) solution in HFE. The emulsion was then visualized in an ibidi u-slide using a confocal laser scanning microscope (Leica, SP8x). The ratio between emissions at 580 and 640 nm was calculated from mean intensities of the same area in both channels. The calibration curve was fitted as a sigmoidal curve. For measuring pH inside shrunk liposomes, the same concentration of SNARF-5F was incorporated in the reaction mixture, consisting of 20 mg/ml lysate, 70 mM K-glutamate, 5 mM Mg-glutamate, 1 U E. coli pyrophosphatase, 1 μM GamS and 7 nM p70a deCFP template. The reaction mixture was then encapsulated in liposomes and shrunk using hypertonic sucrose solutions, to different extent, and imaged.

1.7 Control experiment: Decrease in GFP diffusion at pH close to isoelectric point:

To further verify that the drastic increase we observe in the **No FB, No HEPES** condition is induced by pH close to 6, we performed the same experiment, but with HEPES buffered to pH 6 (**No FB, with HEPES (pH6)** Black diamonds in figure S4). We observe a similar increase in viscosity in this case, indicating that pH close to isoelectric point could explain the drastic increase in viscosity. The trends in viscosity corresponding to **No FB, with HEPES (pH6)** and **No FB, No HEPES** conditions, are not exactly the same, possibly because of high concentration of HEPES (750 mM for lysate concentration 220 mg/ml)

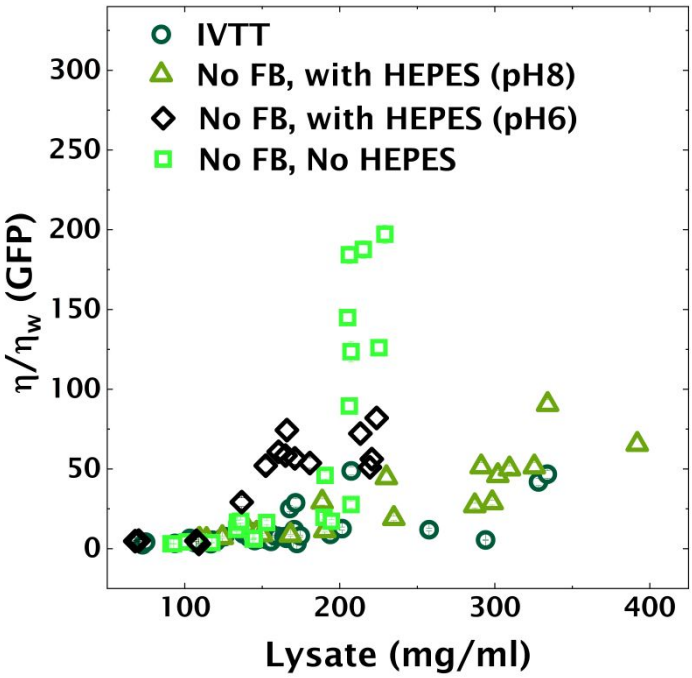

Figure S4. pH close to 6 leads to significant decrease in diffusion, i.e. increase in viscosity, similar to observations in No FB, No HEPES condition. Viscosity experienced by GFP molecules is represented by black diamonds. Corresponding data from figure 2 has been plotted alongside for comparison. The error bars were calculated by error propagation from diffusion coefficients.

1.8 Note on viscosity curves (Figure 2D, S4):

Viscosity was calculated using the Stokes-Einstein equation: $\eta = \frac{k_B T}{6\pi D r}$; where k_B is the Boltzmann's coefficient, T is the temperature, D is the diffusion coefficient and r is the radius of the diffusing particle. For GFP, we used a value of r = 2.82 nm (BNID 104396). We deemed the resulting values to be fairly accurate since GFP is not part of native E. coli proteome, and therefore is not likely to undergo specific interactions with constituents of the cell extract.

The difference in diffusion in the three phases (IVTT; No FB, with HEPES and No FB, no HEPES) is clearly visible in terms of calculated viscosity (Figure 2D) than in diffusion coefficients (Figure 2C) because of two reasons:

1. The drastic decrease in diffusion in No FB, No HEPES arises from a rapid decrease in diffusion coefficients to values <1.

2. Moreover, a ~4-fold decrease in diffusion coefficients e.g. from 1.5 to 0.4 is not clearly visible in Figure 2C, but becomes distinct in calculated viscosity (η/η_W) values which increase 4-fold from ~50 to 200.

2. Effect of cytosolic crowding on gene expression

2.1 Encapsulation and osmotic shrinkage:

Our goal was to determine the effect of cytosolic crowding on gene expression efficiency. Therefore, it was imperative that gene expression was initiated in a crowded environment, rather than in a dilute environment that steadily became crowded over time. To this end, we took advantage of the rapid osmotic shrinkage of partially dewetted liposomes. Upon exposure to hypertonic solution, these liposomes shrink within a few seconds. We captured the liposomes onto a glass slide inside a silicone isolation chamber (SecureSeal, diameter 13 mm, height 0.12 mm). For osmotic shrinkage, 5 µl hypertonic sucrose solution was added. The chamber was then sealed with a coverslip for further observation. Moreover, we imaged only the liposomes at the interface which shrank immediately. In doing so, we were able to study gene expression in liposomes crowded to different extents right from the beginning, and at constant lysate concentration. The number of such liposomes typically varied between 4 to 25. Liposomes farther from the interface shrank slowly as the hypertonic solution diffused through the chamber, and care was taken to avoid measuring protein levels in these liposomes, as the lysate concentration fluctuated in these (increasing gradually over time). The typical duration of the encapsulation process and the subsequent osmotic shrinkage was 5-10 minutes. The liposomes shrink rapidly within a few seconds of contact with hypertonic solution. The amount of deGFP produced in these crowded liposomes was measured exactly 4 hours later.

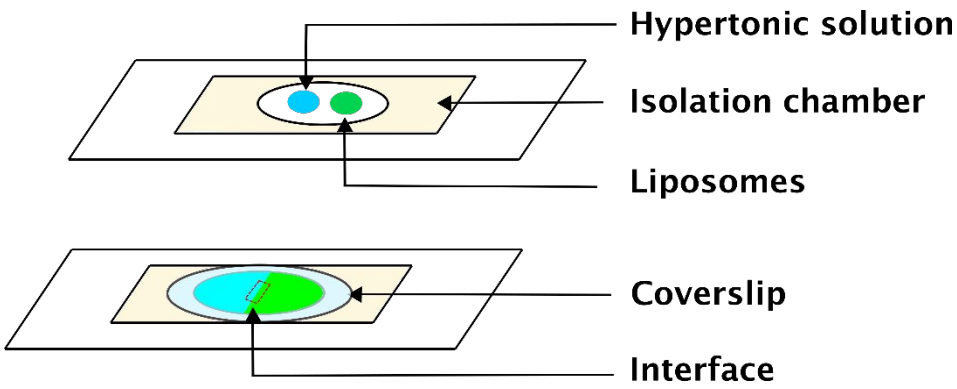

Figure S5. Osmotic shrinkage of partially dewetted liposomes for determining gene expression efficiency as a function of cytosolic crowding. Only the liposomes at the interface which shrank immediately were imaged, to determine protein expression levels at constant lysate concentration.

As the amount of deGFP produced needed to be measured exactly after 4 hours, each experiment yielded 2-3 data points. By repeating the experiment multiple times, with varying concentrations of salts in the IVTT reaction mix and the hypertonic solution, we were able to determine gene expression efficiency as a function of crowding and magnesium.

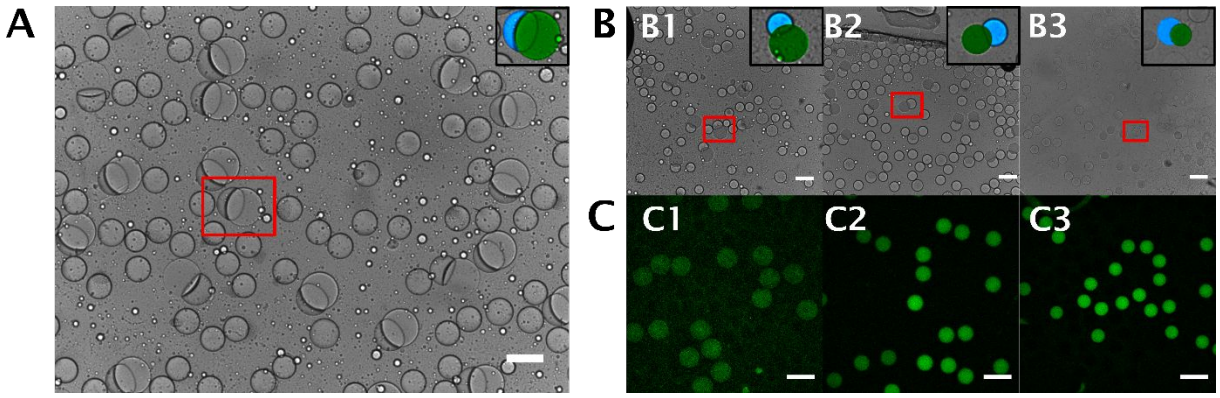

Figure S6. Encapsulation and osmotic shrinkage. (A) Partially dewetted liposomes are monodisperse. (B) Brightfield images of liposomes shrunk with increasing concentration of hypertonic solution; B1-3 were shrunk with 1, 1.5 and 2M sucrose solutions respectively. Insets show false colour images of liposomes highlighted in red box. The blue droplet is the oil phase (5-8 mg/ml egg PC in a mixture of 3:7 v/v chloroform:hexane) and green droplet is the liposome containing IVTT reaction mixture. (C)deGFP expressed in liposomes after 4h. Scale bar 100 µm.

Measurement of concentrations:

After encapsulation, the radii of shrunk and normal liposomes were determined by measuring the area of the liposomes. This was done by first subtracting the background, followed by thresholding. The particle size parameters were then determined by analysing the resulting binary image. The volumes were then determined, and shrinkage factor was calculated. The initial concentrations were then multiplied by the shrinkage factor to determine concentrations in shrunk liposomes.

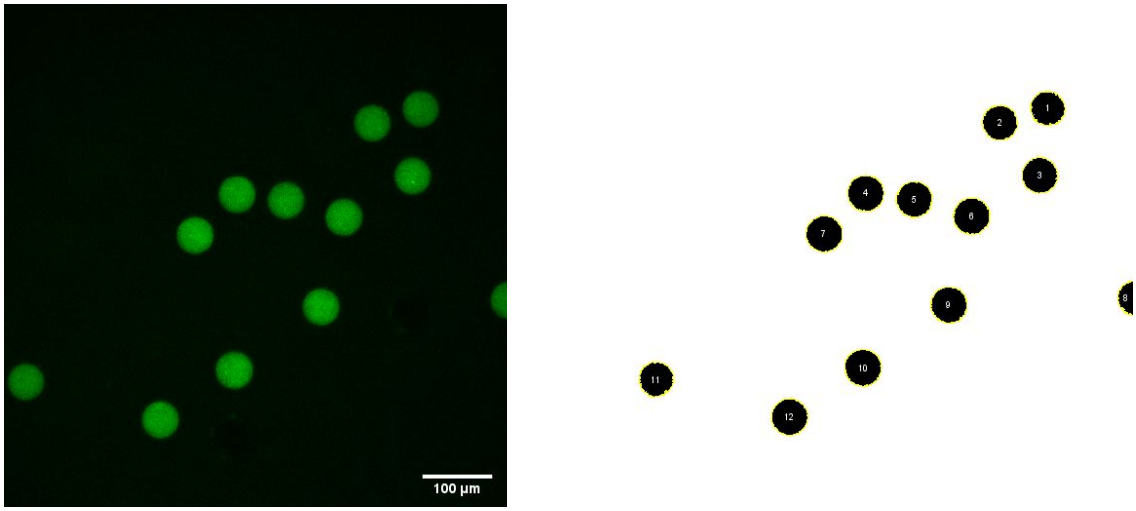

Figure S7. Determination of radius of liposomes by measuring area of liposomes. (A) deGFP fluorescence in liposomes observed with confocal microscope. (B) Thresholded image to determine area, and thereby radius of liposomes.

2.2 Control experiments

We performed a series of control experiments to verify that the variation we observe in expression experiments (Figure 3) is due to the different amount of deGFP produced. eGFP is used instead of deGFP, since their fluorescent properties are the same. deGFP is just more efficiently translated. Shin et al[3] found that translation initiation of eGFP was not efficient in *E. coli*. Therefore they truncated the N-terminal sequence of eGFP according to the work of Li et al[4] and removed ribosome binding site-like sequences.

Buffer conditions have been known to influence the quantum yield of fluorophores. We performed excitation and emission scans of eGFP in varying concentrations of Mg^{2+} in MQ, S30B buffer and IVTT, as well as in varying amounts of lysate, to verify whether we observe a shift in excitation/emission maxima (**Figure S~~2~~8**). We found that, that is not the case.

A. MQ

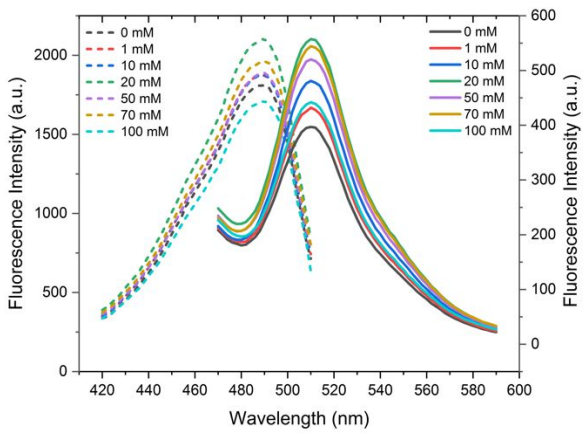

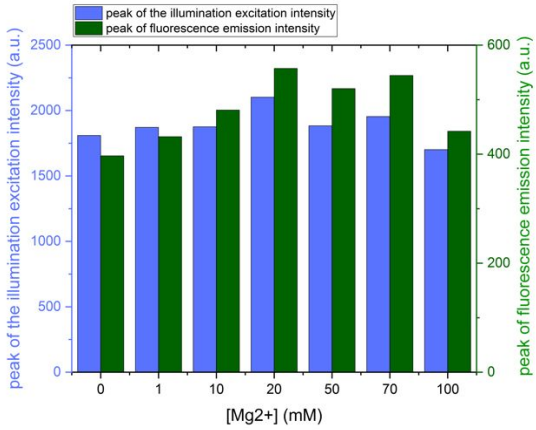

B. S30B

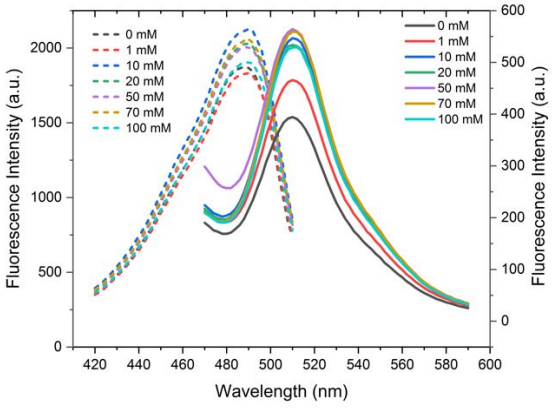

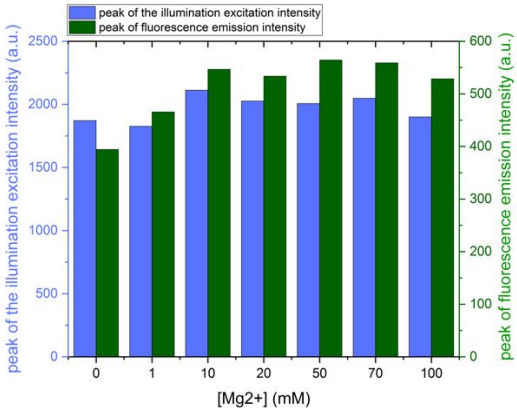

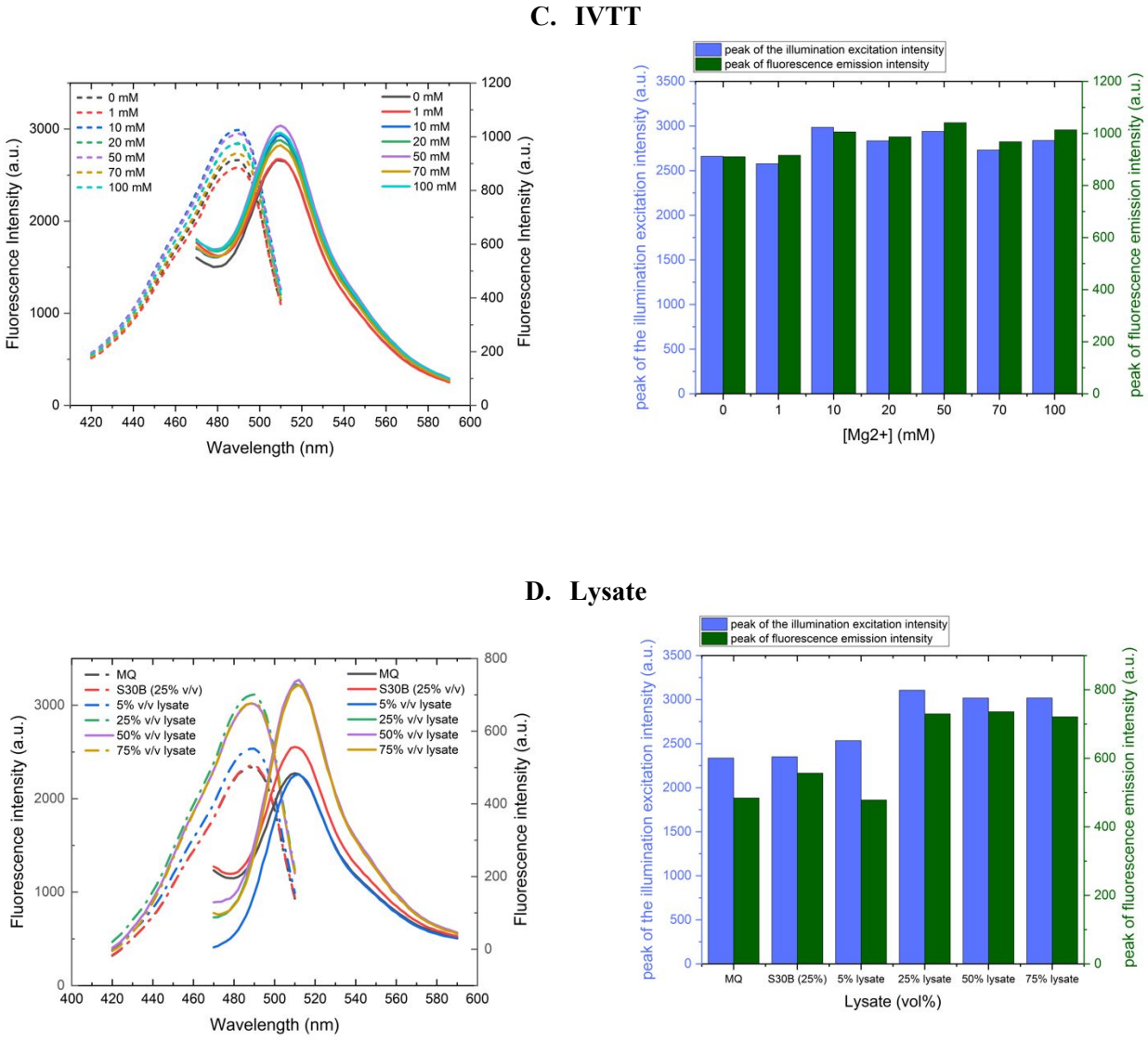

Figure S8. Excitation emission scans of eGFP and corresponding peak values in varying Magnesium concentrations in (**A**) MQ (**B**) 33% v/v S30B buffer (**C**) IVTT and in (**D**) varying lysate concentration.

In case of varying concentration of Mg^{2+} in MQ and S30B buffer (**Figure S~~2~~8A,B**), we find slight variations in the fluorescence output of eGFP, indicating that Mg^{2+} probably has a marginal effect. A similar variation is observed in case of increasing concentration of lysate, although it plateaus after increasing the proportion of lysate beyond 25% v/v (**Figure S~~8~~2D**). However, in case of varying Mg^{2+} in IVTT, even these slight variations are not observed (**Figure S~~2~~8C**). This is probably because most of the Mg^{2+} in the reaction is bound by proteins in lysate, as well as utilized in transcription and translation. These experiments indicate that although Mg^{2+} has a marginal effect on the fluorescence output of eGFP, it is not significant to account for the variation we observed in IVTT in shrunk liposomes.

The next possible source of observed variation was measurement of deGFP in shrunk liposomes. The microfluidic devices we use are handmade, and so, size of liposomes produced with different devices does not remain uniform unlike PDMS devices. This leads to variation in size of liposomes made with different

devices. Variation in initial size of liposomes can result in variation across different experiments. To determine the magnitude of this variation, we performed multiple experiments wherein, we encapsulated eGFP in liposomes, shrunk them to different extents and then measured the total fluorescence intensity (**Figure S9**). Ideally, since the amount of fluorophore remains the same, the total fluorescence intensity should remain the same. However, we do see some variation (CV for total fluorescence intensity is 14%). This translates to CV for volume and so, CV for radius is reduced to 2.4%. This indicates that the variation in initial size of liposome, and subsequent shrinkage is not significant enough to account for the variation we observe in expression experiments (which amounts to CV = 57%).

Data points with similar lysate/magnesium compositions, namely 110/40 and 114/42 or 249/92 and 252/93, might be expected to yield similar amounts of proteins. However, this is not the case and we observe a roughly 30% difference in the amounts of deGFP produced. Part of this variation can be explained by the aforementioned technical reasons. Additionally, both transcription and translation rates vary non-linearly with macromolecular crowding as can be seen in Figure 4C, D, which may lead to amplifications of small initial variations.”

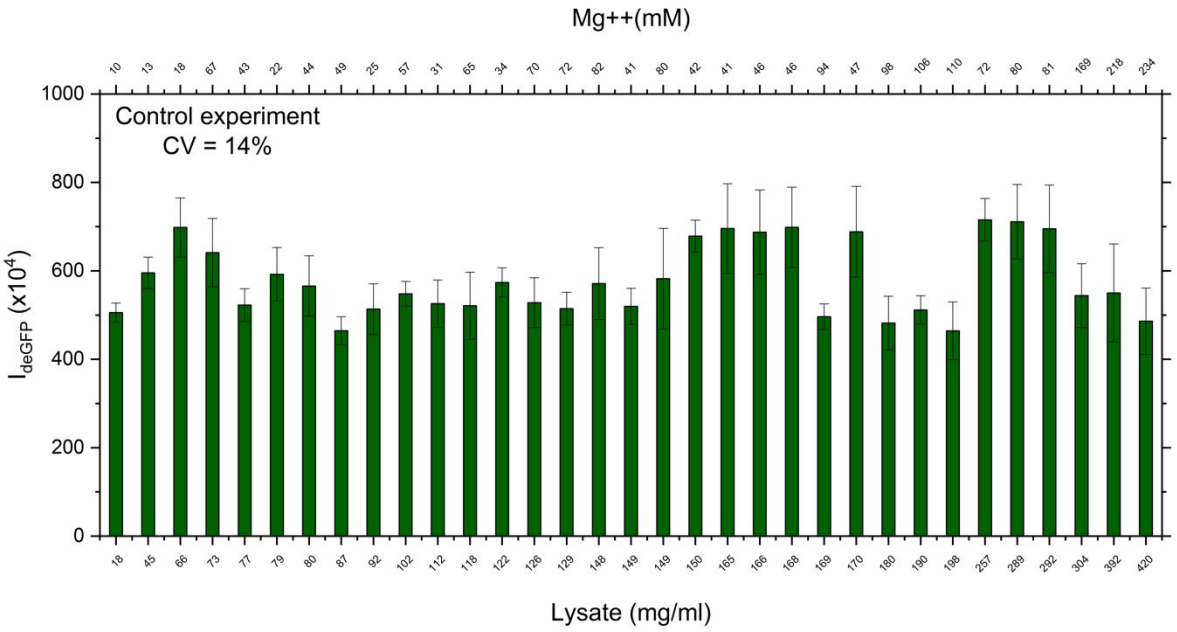

Figure S9. Total fluorescence intensity measurements in liposomes containing eGFP, shrunk to different extents. The error bars indicate SD, when measuring fluorescence in multiple liposomes. The number of liposomes ranged from 8 to 11.

2.3 Lysate autofluorescence correction

E. coli cell lysate has non-negligible autofluorescence upon excitation at 488 nm. In order to increase the accuracy of our measurements, we performed a blank subtraction. We encapsulated the reaction mixture, containing all components of IVTT, except DNA in liposomes and shrank them to different extent. Since the amount (not concentration) of lysate remains constant, the total fluorescence intensity also remains the same. We then averaged these values, and used it as blank value, which we subtracted from expression experiments corresponding to Figure 3.

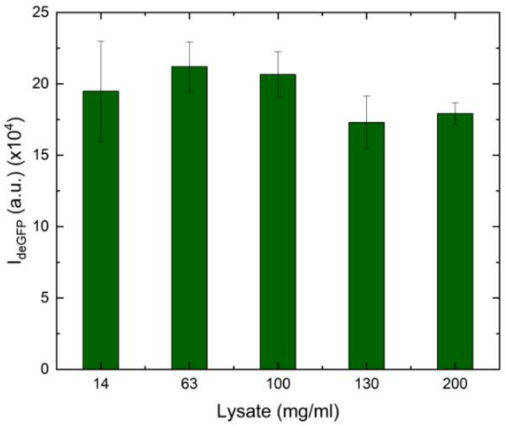

Figure S10. Total fluorescence intensity of blank IVTT (without DNA) in liposomes shrunk to different extents remains roughly the same, indicating that the level of autofluorescence of lysate is constant. The error bars indicate SD, when measuring fluorescence in multiple liposomes. The number of liposomes ranged from 3 to 6.

2.4 Calibration curve

A calibration curve was plotted to determine the amount of deGFP produced inside shrunk liposomes. eGFP is used instead of deGFP, since their fluorescent properties are the same. deGFP is just more translatable. Shin et al[3] found that translation inititation of eGFP was not efficient in *E. coli*. Therefore they truncated the N-terminal sequence of eGFP according to the work of Li et al[4] and removed ribosome binding site-like sequences.

A

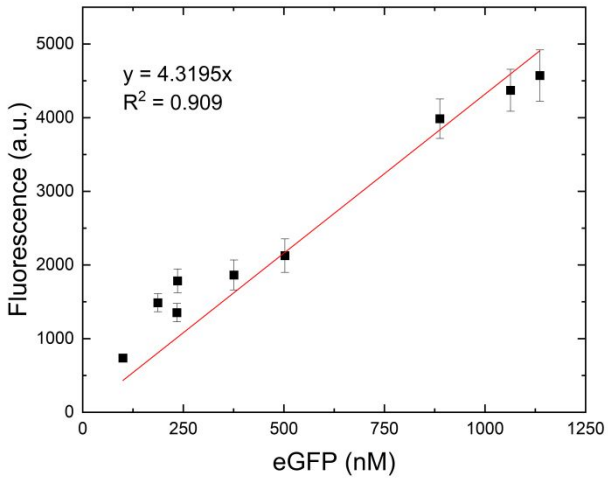

B

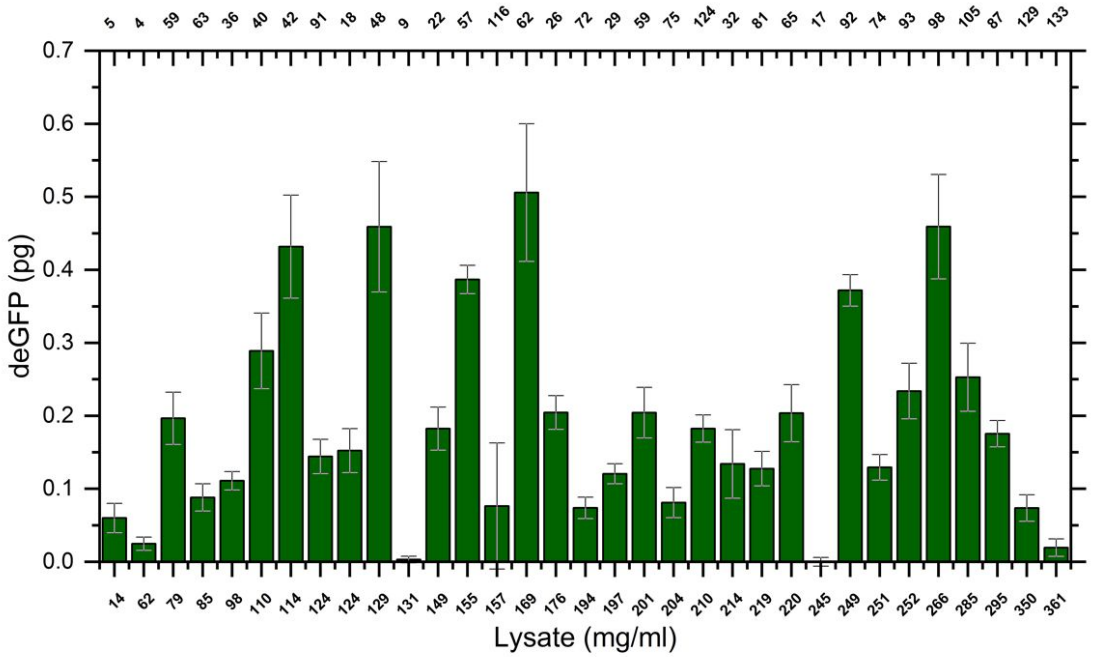

Figure S11. (**A**) Calibration curve. (**B**) Amount of deGFP expressed in shrunk lipospomes determined from the calibration curve. The error bars indicate SD, when measuring fluorescence in multiple liposomes. The number of liposomes corresponding to each lysate concentration ranged from 4 to 23.

Note that at 245 mg/ml (17 mM Mg^{2+}), no expression was observed, and the resulting fluorescence value was slightly less than the blank. This resulted in a negative value after blank subtraction. To avoid this, we simply equated it to zero, as it was close enough to the blank, and performed further calculations.

2.5 Effect of increased NTP concentration

According to Li et al, increasing NTP concentration shifts the optimum magnesium concentration of transcription to higher values. In order to verify this effect, we performed a batch experiment, wherein we performed IVTT with varying magnesium concentrations, in increasing NTP concentrations. Similar to our experiments in liposomes, we used a p70a deGFP template. deGFP was expressed using varying concentrations of magnesium, and increasing NTP concentrations 2 fold and 3 fold: such that final concentrations in these conditions were 3 mM ATP, GTP and 1.8 mM CTP, UTP for 2-fold and 4.5 mM ATP,GTP and 2.7 mM CTP, UTP for 3 fold. We measured deGFP concentration after overnight expression (15h). The optimum magnesium concentration was expected to increase upon increasing NTP concentrations. This was indeed the case.

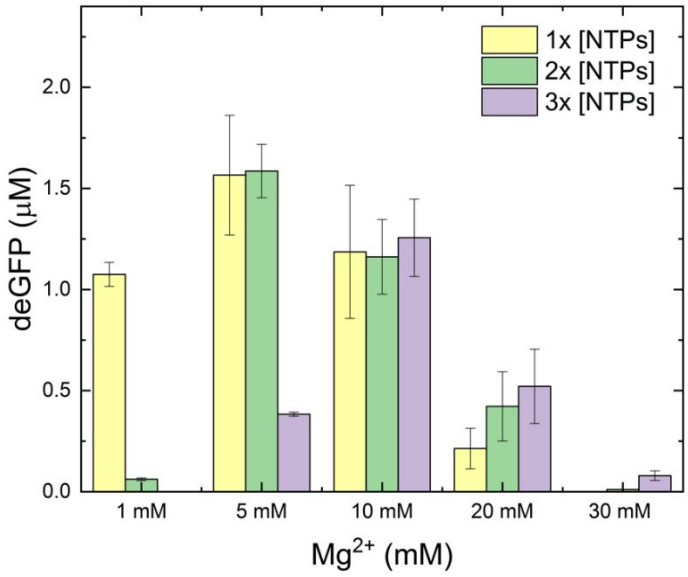

Figure S12. Optimum magnesium concentration shifts to higher values upon increasing NTP concentration. The error bars indicate SD over duplicates.

2.6 Model construction

To check if the model fit would improve if we included two different values for transcriptional and translational resources, we fit our time-lapse data to a modified model where:

$$\frac{dmRNA}{dt} = k_{tx} \cdot M \cdot Res_{tx}$$
$$\frac{dGFP}{dt} = k_{tl} \cdot mRNA \cdot Res_{tl}$$

Res_{tx} and Res_{tl} correspond to the transcription and translation resources respectively. The modified model does not improve the fit compared to the simplified model where $Res_{tx} = Res_{tl} = Res$ (RMSE = 10.1 for both models).

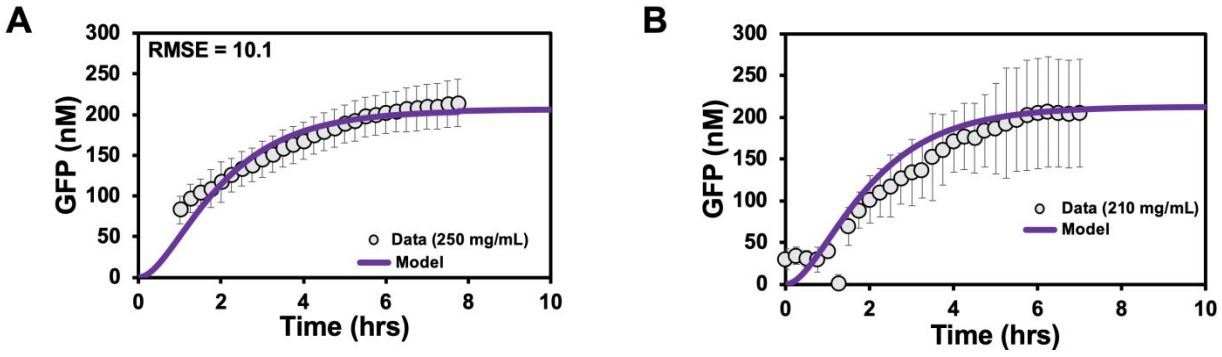

Figure S13. **(A)** Model fit with two different values for Res_{tx} and Res_{tl} at 250 mg/mL. **(B)** Time-laps measurements at 210 mg/mL of lysate compared to our model predictions at these crowding conditions.

To determine the dependency of $\Delta u_{x/l}$ —and thus protein production—on macromolecular crowding conditions, we compared the model to the experimental protein yield for the full range of macromolecular

crowding conditions. We varied the modeled values for Δu_x and Δu_l independently of each other using scaling parameters α and β so that $\Delta u_x = \frac{\alpha}{D_x}$ and $\Delta u_l = \frac{\beta}{D_l}$. $D_{x/l}$ are the crowding dependent diffusion coefficients measured experimentally. We thus systematically altered the scaling parameters α (**Figure S14A**) and β (**Figure S14B**). For eachΔu_x (Figure S15A) and Δu_l value (Figure S15B) we calculated the RMSE of the model (**Figures S14C-D**) and selected values for $\Delta u_{x/l}$ with the lowest RMSE. As a result, values that best fit the experimental data were:

$\ln \Delta u_x = 0.008 \cdot Cr - 0.774$
$\ln \Delta u_l = 0.016 \cdot Cr - 0.473$

Indicated by the bold line in Figure S14A-B.

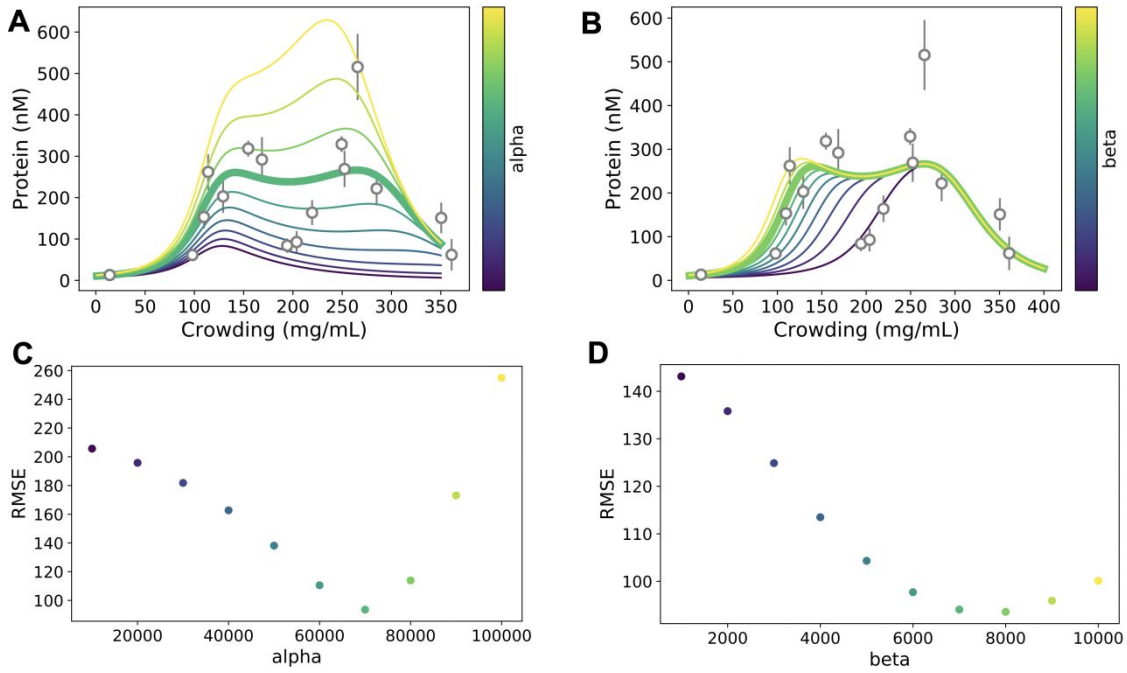

Figure S14. Modeling results show that the first maximum is mostly defined by Δu_l and the second maximum is defined by Δu_x. **(A)** Sensitivity of protein yield after 4 hours to changes in α, where $\Delta u_x = \frac{\alpha}{D_x}$. **(B)** Sensitivity of protein yield after 4 hours to changes in β, where $\Delta u_l = \frac{\beta}{D_l}$. **(A-B)** The values used in Figure 4 for α and β are marked by the bold line and correspond to $\ln \Delta u_x = 0.008 \cdot Cr - 0.774$ and $\ln \Delta u_l = 0.016 \cdot Cr - 0.473$. **(C-D)** RMSE of the respective model fits in panel A and B, showing that the lowest RMSE was selected for both alpha (C) and beta (D).

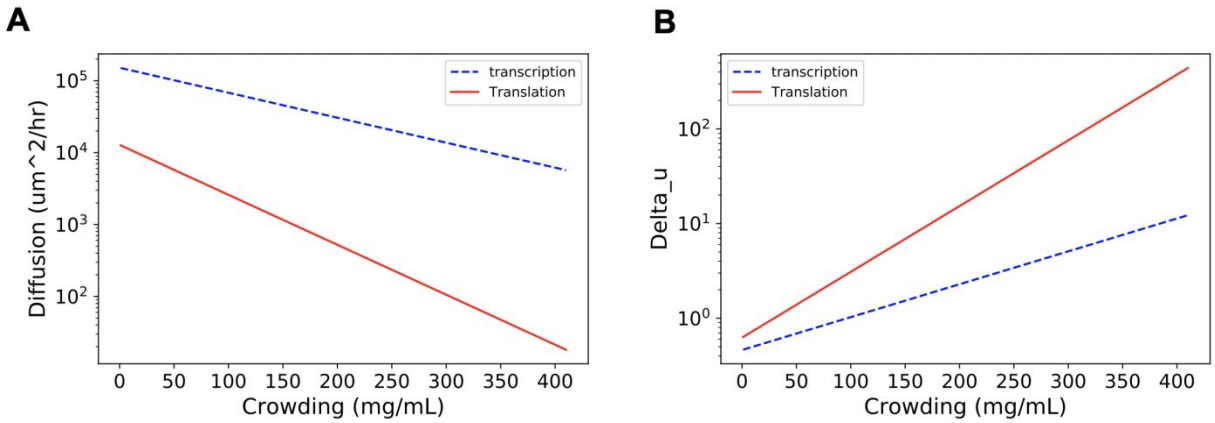

Figure S15. **(A)** Diffusion coefficients of molecules involved in transcription (D_x , blue dashed line) and translation (D_l , red full line) for the macromolecular crowding range. The lines are the respective fits to the experimentally measured diffusion coefficients of GFP (D_x = 151,714 · $e^{-0.008 \cdot Cr}$ μ^2 hr^{-1}) and Ribosomes D_l = 12,833 · $e^{-0.016 \cdot Cr}$ μ^2 hr^{-1}) in Figure 2A. **(B)** $\ln \Delta u_x = 0.008 \cdot Cr - 0.774$ (blue dashed line) and $\ln \Delta u_l = 0.016 \cdot Cr - 0.473$ (red full line) for the macromolecular crowding range (Cr).

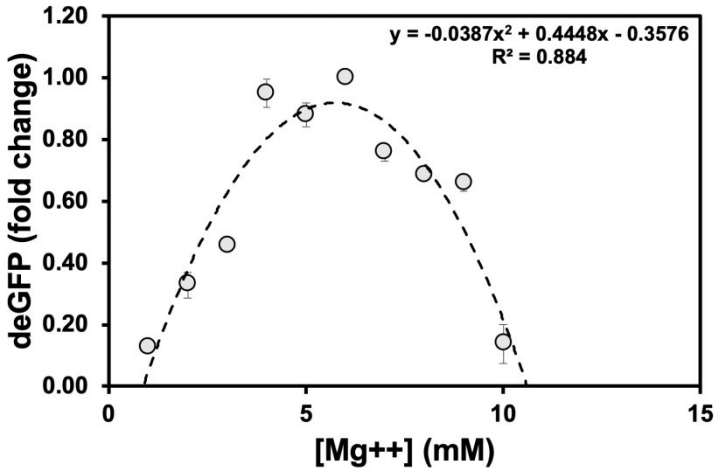

Figure S16. deGFP yields for a range of Mg^{2+} concentrations in bulk conditions. The yield was determined after 15 hours and normalized to the maximum expression at 5mM Mg^{2+}. The fit is a first order polynomial (R^2=0.884). the error bars indicate SD over duplicates.

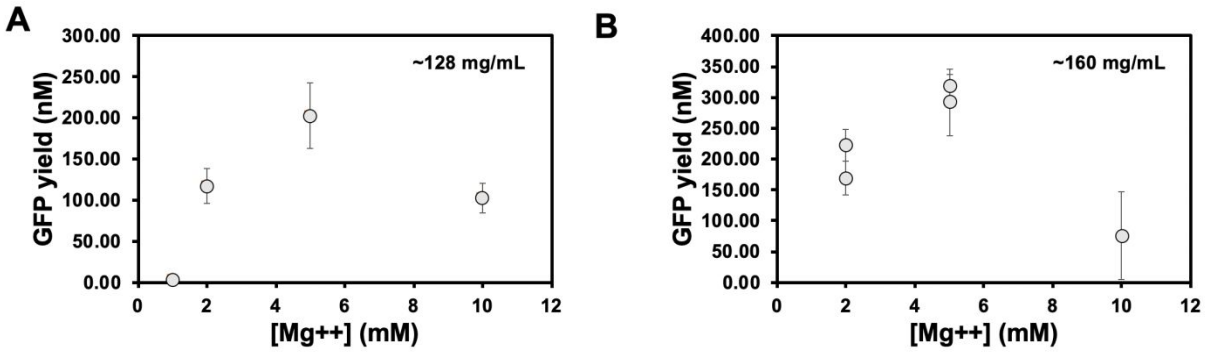

Figure S17. deGFP yields for a range of Mg^{2+} concentrations in shrunk liposomes. The yield was determined after 4 hours and normalized to the maximum expression at 5mM Mg^{2+} across all shrunk liposomes. **(A)** ~ 9-fold shrinkage of liposomes. **(B)** ~11 to 12-fold shrinkage of liposomes. The error bars indicate SD, when measuring fluorescence in multiple liposomes. The number of liposomes corresponding to each lysate concentration ranged from 4 to 23.

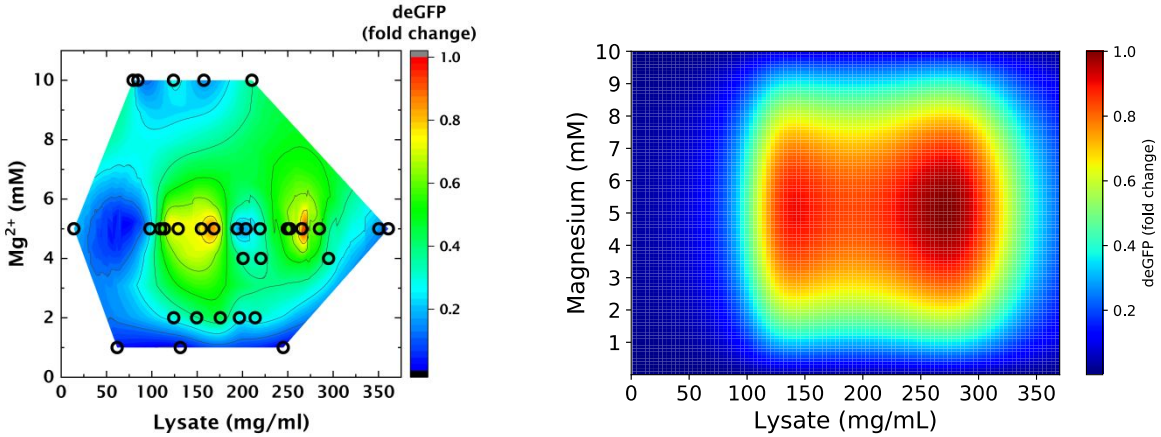

Figure S18. Heatmap showing the fold change in deGFP produced for different amounts of experimental (left) and modeled (right) macromolecular crowding and starting [Mg^{2+}], independent of the degree of liposome shrinkage.

3. References

(1) Blanchard, S. C., Kim, H. D., Gonzalez, R. L., Puglisi, J. D., and Chu, S. (2004) tRNA dynamics on the ribosome during translation. *Proc. Natl. Acad. Sci. U. S. A. 101*, 12893–8.

(2) Thiele, J., Ma, Y., Foschepoth, D., Hansen, M. M. K., Steffen, C., Heus, H. A., and Huck, W. T. S.

(2014) DNA-functionalized hydrogels for confined membrane-free in vitro transcription/translation. *Lab Chip 14*, 2651.

(3) Shin, J., and Noireaux, V. (2010) Efficient cell-free expression with the endogenous E. Coli RNA polymerase and sigma factor 70. *J. Biol. Eng. 4*, 8.

(4) Li, X., Zhang, G., Ngo, N., Zhao, X., Kain, S. R., and Huang, C. C. (1997) Deletions of the Aequorea victoria green fluorescent protein define the minimal domain required for fluorescence. *J. Biol. Chem. 272*, 28545–9.